Plant Soil
https://doi.org/10.1007/s11104-026-08273-5

RESEARCH ARTICLE

A novel mechanism of plant defense induction by *Trichoderma hamatum* via cell wall-derived elicitors from *Sclerotinia sclerotiorum*

Pablo Velasco · Rosaura Abilleira · María Díaz-Urbano · Jorge Poveda

Received: 13 June 2025 / Accepted: 2 January 2026

Abstract

Aims *Trichoderma* is a filamentous fungus beneficial to crops and widely used as biofungicide. Its mechanisms of action as a biological control agent against phytopathogenic fungi include mycoparasitism and the induction of plant defense responses. On the other hand, *Sclerotinia sclerotiorum* is an important pathogen for *Brassica* crops, effectively suppressed by *Trichoderma*. The aim of this work is to determine whether *T. hamatum* can release elicitors from the cell wall of *S. sclerotiorum* that activate plant systemic defenses against the pathogen.

Methods Liquid fermentation of *T. hamatum* on *S. sclerotiorum* mycelium was performed. In the resulting fungal filtrates, chitinase and β-endoglucanase activities were quantified, along with the amounts of glucosamine and glucan oligomers produced. These filtrates were subsequently applied to the roots of broccoli plants (*Brassica oleracea* var. *italica*), which were later foliar-infected with the pathogen. Lesions produced were measured and different systemic defensive responses were evaluated through hormonomics, glucosinolate profiling and non-targeted metabolomics.

Results In fungal filtrates of *T. hamatum* cultured on *S. sclerotiorum*, chitinase (7.56–8.32 units/mL) and β-endoglucanase (3.45 units/mL) activity was determined. These filtrates also contained the highest amounts of glucosamine (0.75 g/L) and glucan oligomers (43.8 g/L). When applied to broccoli plants, the filtrates triggered a systemic defense response that was effective against the pathogen. This response was mediated by the hormones jasmonic acid, isopentenyladenine and ethylene, leading to the accumulation of antifungal compounds in the leaves, including glucobrassicin, niacin and several fatty acids. This defensive induction was not observed with glucosamine oligomers.

Conclusions Therefore, *T. hamatum* releases glucan oligomers from the cell wall of *S. sclerotionum* which may act as potential elicitors of systemic plant defenses.

Highlights

• *T. hamatum releases oligomers from the S. sclerotiorum cell wall by enzymatic action.*

• Glucan oligomers, but not glucosamine oligomers, induce systemic plant resistance.

• Systemic resistance is mediated by ethylene/jasmonic acid, a response to necrotrophs.

Responsible Editor: Stijn Spaepen.

P. Velasco (✉) · R. Abilleira · M. Díaz-Urbano
Group of Genetics, Breeding and Biochemistry of Brassicas, Mision Biologica de Galicia (MBG-CSIC), 36143 Pontevedra, Spain
e-mail: pvelasco@mbg.csic.es

J. Poveda (✉)
Recognised Research Group AGROBIOTECH, UIC-370 (JCyL), Department of Plant Production and Forest Resources, Higher Technical School of Agricultural Engineering of Palencia, University Institute for Research in Sustainable Forest Management (iuFOR), University of Valladolid, Avda. Madrid 57, 34004 Palencia, Spain
e-mail: jorge.poveda@uva.es

Published online: 22 January 2026

• Reduced *S. sclerotiorum*-foliar infection is due to an accumulation of glucobrassicin and niacin.
• *Trichoderma* is able to release plant defense elicitors from the pathogen cell wall.

Keywords β-glucanase · β-glucan · Ethylene and jasmonic acid · Broccoli · *Trichoderma*

Introduction

Fungal-plant interactions are believed to have originated approximately 450–460 million years ago, forming symbiotic relationships (with mycorrhizal fungi and endophytic fungi) (Priyashantha et al. 2023). In contrast, the interaction between plants and phytopathogenic fungi emerged later, initiating a co-evolutionary arms race in which plants evolved mechanisms to defend against pathogens, while fungi developed strategies to evade plant defenses (Priyashantha et al. 2023). In both symbiotic and phytopathogenic fungal interactions, a complex molecular dialogue is established, wherein both the plant and the fungus recognize each other's molecular signals and elicit corresponding physiological response. Plants detect the presence of fungi through pattern recognition receptors (PRRs) located on the plasma membrane, which recognize pathogen-associated molecular patterns (PAMPs) (from pathogen-cells) or microbe-associated molecular patterns (MAMPs) (from symbiotic-cells). This recognition triggers local and systemic defense responses in the plant (Priyashantha et al. 2023). These plant defenses are also activated in response to mycorrhizal and endophytic fungi. However, to facilitate colonization by symbiotic fungi, plants must temporarily suppress their immune responses (Almario et al. 2022). Moreover, plant immune responses can influence the type of symbiotic relationships that are established. For example, members of the Brassicaceae family are unable to form effective mycorrhizal associations due to the presence of glucosinolates (GSLs) in their tissues, yet they can establish beneficial interactions with various endophytic fungi (Poveda et al. 2022).

Pathogens also interact with the Brassicaceae family, among which the fungus *Sclerotinia sclerotiorum* stands out as one of the world's most virulent and widespread plant pathogen. This fungus causes the so-called stem rot in brassicas, entering the plant through any of its aerial organ or via the soil. The disease can cause severe losses in *Brassica* crops, accounting for up to 80% of annual losses in global oilseed rape production (Hossain et al. 2023; Shang et al. 2024). To successfully infect brassicas, *S. sclerotiorum* must be able to overcome the plant's constitutive and inducible defenses. Therefore, a continuous plant-fungus molecular recognition occurs (Chen et al. 2023). Disease management strategies include cultural practices (crop rotation, reducing plant density, burning crop residues or using irrigation to increase rotting of sclerotia), plant resistance (resistant cultivars or molecular breeding), chemical fungicides (anilinopyrimidines, methyl benzimidazole carbamates or dicarboxamides) and the use of bacterial (*Bacillus* spp. or *Streptomyces* spp.), fungal (*Coniothyrium minitans* or *Trichoderma* spp.) and/or mycovirus biological control agents (BCAs) (O'Sullivan et al., 2021).

One of the most widely studied and used BCAs in agriculture is the fungal genus *Trichoderma*, which is broadly distributed across diverse ecosystems and climatic regions (Afzal et al. 2021). Species within this genus have been recognized as effective biofertilizers, due to their ability to promote plant growth through nutrient solubilization and chelation (P, Fe, Mg, Mn), production of phytohormones (auxins) and modulation of the rhizospheric microbiota (Gupta 2020). Certain *Trichoderma* species also enhance plant tolerance to abiotic stresses by mitigating oxidative stress and altering gene expression, as well as through direct mycoremediation on pollutants and heavy metals (dos Santos et al. 2022). However, the primary agricultural interest of *Trichoderma*-based bioinoculants lies in their role as BCA, accounting for up to 60% of the current biofungicides on the world market (Kubiak et al. 2023). In recent years, their application as bionematicides (TariqJaveed et al. 2021) and bioinsecticides (Poveda 2021) has also gained increasing attention.

The mechanisms of action involved in the action as BCA of different *Trichoderma* species include mycoparasitism, antibiosis, competition for space and nutrients, and activation of plant defenses (Guzmán-Guzmán et al. 2023). Specifically, mycoparasitism is based on the ability of *Trichoderma* to degrade the cell wall of phytopathogenic fungi and extract nutrients from within. To achieve this, they use cell wall-degrading enzymes (CWDEs), mainly

chitinases, glucanases and proteases (Mukherjee et al. 2022; Dutta et al. 2023). The key CWDEs produced by *Trichoderma* to destroy the cell wall of pathogenic fungi are endochitinase, β−1,3 glucanase and chitobiosidase (Wang et al., 2024; Shahbazi et al. 2025). The lytic action of these enzymes releases oligomers (oligosaccharides and oligopeptides), from fungal walls, which are recognized by *Trichoderma*, thereby triggering the upregulation of additional antifungal genes (Karlsson et al. 2017). Through the mechanism known as antibiosis, *Trichoderma* produces and releases various low-molecular-weight volatile and diffusible compounds with antimicrobial properties. These compounds include azaphilones, butenolides, trichothecenes, pyrones, lactones, polyketides or peptaibols (Maurya et al. 2024). In addition, *Trichoderma* exhibits rapid and robust growth on a variety of substrates, enabling it to outcompete phytopathogens for space and nutrients within the rhizosphere. This competitive advantage is partly attributed to its efficient nutrient acquisition strategies, such as iron sequestration via siderophore production (Amerio et al. 2024). Finally, *Trichoderma* can activate both local and systemic plant defense mechanisms. Recognition of microbe-associated molecular patterns (MAMPs) from *Trichoderma* by the host plant initiates a signaling cascade involving key defense-related hormones, notably salicylic acid (SA), jasmonic acid (JA), and/or ethylene (ET). This signaling leads to the synthesis and accumulation of various antimicrobial proteins and secondary metabolites, enhancing the plant's resistance to subsequent pathogen attacks (Khan et al. 2023).

Specifically, *Trichoderma hamatum* has been recently studied in a specific review highlighting its diverse functional capabilities, including plant growth promotion, antimicrobial and antioxidant activity, insecticidal and herbicidal properties, as well as its potential for mycoremediation (Lodi et al. 2023). *T. hamatum* H690 strain, used in this study, was previously described as a biofertilizer and agricultural product quality improver in leafy brassica crops (Velasco et al. 2021). Additionally, it has demonstrated bioinsecticidal activity against the lepidopteran *Spodoptera littoralis* (Lana et al. 2023); and has been proposed to function as an interplant signaling mediator, facilitating communication between neighboring plants (Poveda et al. 2023).

The mycoparasitic interaction between *Trichoderma* and *S. sclerotiorum* has been described in several works. Various *Trichoderma* species are able to mycoparasitize both hyphae and sclerotia of *S. sclerotiorum*, leading to their complete degradation. This antagonistic activity is primarily mediated by the secretion of CWDEs, including endochitinases, α-glucanases and β-glucanases (Ojaghian et al. 2020; Tomah et al. 2024).

Elicitors are microbial molecules released by or present in pathogens, called PAMPs, which are recognized by specific receptors on host plant cells, triggering their defenses or PAMP-triggered immunity (PTI). These elicitors include lipids, oligosaccharides, peptides and proteins. Among the most prominent PAMPs found in pathogenic fungi chitin/chitosan, β-glucans or ergosterol (Abdul-Malik et al. 2020; Meena et al. 2022). Specifically, chitosan act as an elicitor by enhancing nitric oxide production and stimulating the activity of reactive oxygen species (ROS)-scavenging enzymes in plant tissues (Stasińska-Jakubas et al., 2022). Similarly, β-glucans can induce the accumulation of phytoalexins and/or the deposition of callose (Frolova and Berestetskiy 2024).

In this context, the main objective of this work was to determine whether *T. hamatum* can release elicitor molecules from the cell wall of *S. sclerotiorum* that activate plant systemic defenses. For this purpose, co-cultivation experiments involving various combinations of both fungi were conducted in liquid fermentation systems. Chitinase and glucanase activities were measured in the resulting cultures, along with the quantification of released oligomers. In broccoli plants, systemic defense responses against foliar infection by *S. sclerotiorum* were evaluated through hormonal profiling, GSLs analysis and non-targeted metabolomics. Therefore, the work has been developed based on the hypothesis that *T. hamatum* is capable of degrading the cell wall of *S. sclerotiorum* and releasing oligomers that function as elicitors of systemic plant immunity.

Material and Methods

Fungal and plant material

T. hamatum H690 was previously isolated from roots of kale (*Brassica oleracea* var. *acephala*) in a

previous work with different local populations from Galicia (Northwestern Spain) (Poveda et al. 2020). *S. sclerotiorum* MBG-Ss2, collected from a naturally infected plant of oilseed rape (*Brassica napus*) in an experimental field of the Biological Mission of Galicia (MBG, Northwestern Spain) (Madloo et al. 2021), was used as a soil and aerial pathogenic fungus. Both fungal strains were routinely grown on potato-dextrose-agar (PDA, Sigma-Aldrich, Madrid, Spain) in the dark at 25 °C.

The plant used was the doubled haploid broccoli line "Early Big" (*B. oleracea* var. *italica*), in order to minimize variability in plant responses to the different treatments. Seeds were obtained from the *Brassica* germplasm bank of the MBG's.

Fungal fermentation

The liquid culture of *T. hamatum* and *S. sclerotiorum* was performed following the methodology previously described by Lana et al. (2023), with minor modifications. The culture medium used was 50 mL of potato dextrose broth medium (PDB, Sigma-Aldrich, Madrid, Spain) on an orbital shaker at 150 rpm and 25 ºC. Table 1 shows the different liquid fermentations carried out to obtain the extracts used as plant treatments. All fermentations were carried out in 10 independent biological replicates and incubated for 72 h. After incubation, cultures were filtered through sterile 0.2 µm filters (Sigma-Aldrich, Madrid, Spain). The resulting filtrates were stored at − 20 °C until further use.

Chitinase and glucanase activity analysis

Chitinase and glucanase activity analysis was performed on the different fungal filtrates. Chitinase activity was quantified following the methodology previously described by Lana et al. (2023). From each set of 10 filtrates obtained per fungal fermentation, 50µL aliquots were used to measure chitinase enzyme activity, using the commercial Chitinase Assay Kit (Sigma-Aldrich, Madrid, Spain), which enables quantification of endochitinase and exochitinase activities (chitobiosidase and β-N-acetylglucosaminidase). The analysis is based on the enzymatic hydrolysis of different substrates at 4.8 pH, releasing p-nitrophenol, which can be quantified colorimetrically at 405 nm (Multiskan SkyHigh Microplate Spectrophotometer; Thermo Fisher, Waltham, USA). The substrates used were 4-Nitrophenyl N,N′-diacetyl-β-D-chitobioside (chitobiosidase activity), 4-Nitrophenyl N-acetyl-β-D-glucosaminidase (β-N-acetylglucosaminidase activity), and 4-Nitrophenyl β-D-N,N′,N‴-triacetylchitotriose (endochitinase activity). Enzyme activities are expressed as units/mL. All analyses were performed in triplicate from the different fungal filtrates.

β-Endoglucanase enzyme activity was measured using a modified version of the method described by

Table 1 Different liquid fermentations carried out to obtain fungal extracts used as plant treatments

ACRONYM	DESCRIPTION
PDB	Culture medium only
PDB + Q	Culture medium with 0.75 g (1,5% w/v) of chitin
PDB + Th	Culture medium inoculated with 2.5×10^6 spores/mL of *T. hamatum*
PDB + Q + Th	Culture medium with 0.75 g chitin, inoculated with *T. hamatum* spores (2.5×10^6 spores/mL)
PDB + Ss	Culture medium inoculated with a sclerotium of *S. sclerotiorum*
PDB + Ss + Th	Culture medium with 0.75 g of PDB + Ss mycelium (after 72 h of culture) washed, filtered and autoclaved* and re-washed, inoculated with *T. hamatum* spores (2.5×10^6 spores/mL)
(PDB + Ss) + (PDB + Th)	Filtered cultures of PDB + Ss and PDB + Th mixed 50/50
(PDB + Ss) + (PDB + Q + Th)	Filtered cultures of PDB + Ss and PDB + Q + Th mixed 50/50

Q: chitin from shrimp shells (Sigma-Aldrich, Madrid, Spain)

*The *S. sclerotiorum* mycelium is autoclaved so that *T. hamatum* grows only on pathogen tissues, without the pathogen continuing to grow

Zantinge et al. (2002). The substrate used to measure fungal β-endoglucanase activity was 0.2% azurine dye co-valently cross-linked (AZCL)-hydroxyethyl-cellulose (HE) (Megazyme, Ireland), dissolved in 25 mM sodium acetate (pH 4.5), with 2% agar added. The mixture was autoclaved and dispensed into 96-well microplate wells. After solidification, 50 µL of the 10 different fungal filtrates were added to each well, along with 25 mM sodium acetate (pH 4.5) to a final volume of 350 µL. Microplates were incubated overnight at room temperature. β-Endoglucanase activity was determined by the release of a blue color from the hydrolysis of AZCL-HE, which was quantified colorimetrically at 590 nm (Multiskan SkyHigh Microplate Spectrophotometer; Thermo Fisher, Waltham, USA). Enzyme activity was expressed in units/mL, calculated using the formula: Units/mL = [(Absorbance-0.02)/0.911]. All analyses were performed in triplicate from the different fungal filtrates.

Chitin and glucan oligomers quantification

To quantify the chitin oligomers released in the various fungal filtrates, a modified version of the method described by Katano et al. (2016) was employed. The substrate solution consisted of mixing 5 mL of 0.1 mol/L sodium metasilicate (Na_2SiO_3), and 1.2 mol/L isodium molybdate dihydrate (Na_2MoO_4) in water, with 3 mL of dimethyl sulfoxide (DMSO). Subsequently, 1.5 mL 10 mol/L acetic acid in water and 3.5 mL of water were added to the mixture, which was then allowed to stand for 30 min. For the quantification reaction, 200 µL of the prepared substrate solution were added to each microwell, followed by 20 µL of the respective fungal filtrate. The amount of chitin oligomers was expressed in g/L glucosamine by measuring absorbance at 750 nm (Multiskan SkyHigh Microplate Spectrophotometer; Thermo Fisher, Waltham, USA). All analyses were performed in triplicate for each fungal filtrate.

On the other hand, glucan oligomer quantification was carried out following the method described by Kupetz et al. (2017). This methodology was based on Congo red staining, using the Gluca-test rapid test kit (R-biopharm, Germany). In 15 mL tubes, 200 µL of each fungal filtrates were mixed with 3 mL of the reaction solution provided in the kit. The mixture was incubated for 30 min and distributed on a 96-well microplate wells for absorbance measurement at 550 nm at (Multiskan SkyHigh Microplate Spectrophotometer; Thermo Fisher, Waltham, USA). The concentration of β-glucans was expressed in mg/L. All measurements were performed in triplicate for each fungal filtrate.

In planta assays

Broccoli plant growth and leaf infection were assessed using a modified version of the methodology described by Rodriguez et al. (2023), with modifications. Broccoli seeds were surface sterilized by shaking them in 70% ethanol solution for 15 min, 5% sodium hypochlorite solution for 5 min, and then rinsing four times with autoclaved distilled water. The sterilized seeds were sown in 0.5 L pots with peat moss (Profi-Substract, Gramoflor, Valencia, Spain) previously sterilized in an autoclave (twice, 24 h apart) as culture substrate. Plants were maintained in a greenhouse under the following conditions throughout the experiment: 14 h photoperiod, ambient temperature (12–30 °C), and relative humidity above 80%. No exogenous fertilizers were applied. Plants were irrigated 2–3 times per week, based on visual assessment of water needs, ensuring equal volumes of water were applied to all plants.

When the plants had developed their third true leaf, they were treated with the six different fungal filtrates by applying 1 mL of each filtrate directly to the main root using a pipette tip. Fifteen plants were treated with each fungal filtrate. The assay was repeated three times.

Forty-eight hours after application of the fungal filtrates, foliar infection with *S. sclerotiorum* was performed on the middle portion of the third true leaf of each plant. For inoculation, 6 mm agar plugs were excised from the actively growing edge of fungal colonies cultured on Petri dishes. Leaf infection was conducted by applying 5 µl of sterile agarose as "a glue" for the fungal plug to each leaf and placing the fungal mycelium in contact with the leaf surface. Seventy-two hours post-infection, photographs were taken to assess lesion development, and plant samples were collected for biochemical analysis.

Lesion area of each leaf was quantified using ImageJ software (US National Institutes of Health, Bethesda, U.S.A.). For biochemical analysis, tissue samples were collected separately from the infected leaf and the remaining aerial parts of the plant. All

plant material was immediately frozen in liquid nitrogen and stored at −80ºC until processing. Subsequently, this plant material was freeze-dried and pulverized.

Hormone profiling

Hormonal analysis was performed on five pooled samples, each comprising the aerial parts of three plants infected with *S. sclerotioum* (Ss) and previously root-inoculated with either PDB or PDB + Ss + Th treatments. For the study of the hormonal profile of the samples, the methodology previously described by Albacete et al. (2008) was used, with some modifications. A total of 0.05 g of powdered plant material was incubated for 30 min at 4 °C in 1 mL of cold (− 20 °C) extraction solution consisting of methanol/water (80/20, vol/vol). Following incubation, the mixture was centrifuged at 20,000 × g for 15 min at 4 °C to separate the solids. A second extraction was then performed under the same conditions using an additional 1 mL of extraction solution. The combined supernatants were passed through Sep-Pak Plus C18 cartridges (which had been pre-conditioned with 3 mL of extraction buffer) to remove lipids and pigments. The resulting supernatants were evaporated under vacuum at 40 °C. The residue was re-dissolved in 1 mL of methanol/water (20/80, vol/vol) solution using an ultrasonic bath. The reconstituted samples were then filtered through 13-mm Millex filters with a 0.22-µm nylon membrane (Millipore, Bedford, MA) and transferred to opaque microcentrifuge tubes. A 10 µL aliquot of the filtered extract was injected into an Accela Series UHPLC system (ThermoFisher Scientific, Waltham, MA) coupled to an Exactive mass spectrometer (ThermoFisher Scientific, Waltham, MA) via a heated electrospray ionization (HESI) interface. Mass spectra were acquired using Xcalibur software version 2.2 (ThermoFisher Scientific, Waltham, MA). Quantification of hormones was carried out using calibration curves generated for each compound at concentrations of 1, 10, 50, and 100 µg/L, and corrected with 10 µg/L deuterated internal standards. Recovery rates ranged between 92 and 95%.

For chromatographic separation, 8 µl of each sample, previously dissolved in mobile phase A, was injected into a Zorbax SB-C18 HPLC column (5 µm, 150 × 0.5 mm; Agilent Technologies, Santa Clara, CA, USA). The column was maintained at a constant temperature of 40 °C, and separation was performed at a flow rate of 10 µl/min. Chromatographic separation utilized mobile phase A (water/acetonitrile/formic acid in a 94.9:5:0.1 ratio, v/v) and mobile phase B (water/acetonitrile/formic acid in a 10:89.9:0.1 ratio, v/v). The elution program began with 100% A for 5 min, followed by a linear gradient increasing B from 0 to 6% over 10 min. This was continued by a second gradient from 6 to 100% B over 5 min, with a final hold at 100% B for 5 additional minutes. Prior to each analysis, the column was re-equilibrated with the initial mobile phase composition for 30 min. Detection was performed at 280 nm using a DAD detector module (Agilent Technologies, Santa Clara, CA, USA).

GSLs analysis

The GSLs profile was analyzed in the fifteen *S. sclerotiorum*-infected leaves of plants previously treated at the root level with various fungal filtrates. GSLs analysis was performed on the freeze-dried and powdered plant material, following the methodology previously described by Poveda et al. (2021), with minor modifications.

Quantification of GSLs was performed using an Ultra High Performance Liquid Chromatograph (UHPLC) Nexera LC-30AD from Shimadzu Corporation (Kyoto, Japan). This system was fitted with a Nexera SIL-30AC injector and a SPDM20A UV/VIS photodiode array detector, both from Shimadzu. For the analysis, an X Select® HSS T3 UHPLC column (2.5 µm particle size, 2.1 mm inner diameter, and 100 mm in length) was utilized, provided by Waters Corporation in Milford, MA, USA, along with a VanGuard pre-column. The oven temperature was maintained at 35ºC, and the GSLs were quantified at a wavelength of 229 nm.

Separation was achieved using the aqueous acetonitrile method. Identification of individual GSLs was based on comparison of retention times and UV spectra against standards from Phytoplan Diehm & Neuberger GmbH (Heidelberg, Germany). Calibration equations for each GSL were established using a minimum of five data points: glucoiberin (GIB) ($y = 99397x$; $R^2 = 0.950$), glucoraphanin (GRA) ($y = 352910x$; $R^2 = 0.999$), glucobrassicin (GBS) ($y = 869483x$; $R^2 = 0.988$), neoglucobrassicin (NEOGBS) ($y = 342954x$; $R^2 = 0.997$), and methoxyglucobrassicin (MEOGBS) ($y = 398645x$; $R^2 = 0.980$).

Metabolomic analysis

Untargeted metabolomics analysis of *S. sclerotiorum*-infected leaves was conducted following the methodology previously described by Poveda et al. (2021), with minor modifications. A 50 mg sample of freeze-dried powder was dissolved in 500 mL of 80% methanol in water and sonicated for 15 min. The mixture was then centrifuged for 10 min at 16,000 × g and room temperature. The resulting supernatant was then filtered through a 0.20 µm PTFE micropore membrane and stored in vials for subsequent analysis.

Metabolomic profiling was performed using ultra-high-performance liquid chromatography (UPLC) coupled with electrospray ionization quadrupole time-of-flight mass spectrometry (UPLC-Q-TOF–MS/MS). The system consisted of a Thermo Dionex Ultimate 3000 LC system (Thermo Fisher Scientific, Waltham, MA, USA) and a Bruker Compact™ mass spectrometer with a heated electrospray ionization (ESI) source. Chromatographic separation was achieved on a 2.1 × 100 mm 1.7 µm Intensity Solo 2 C18 column (Bruker Daltonics, Billerica, MA, USA).

The mobile phase consisted of 0.1% formic acid in water (solvent A) and acetonitrile (solvent B) in a binary gradient. The gradient profile was as follows: 3% B for 0–4 min, increasing from 3 to 25% B from 4 to 16 min, from 25 to 80% B between 16 and 25 min, from 80 to 100% B from 25 to 30 min, holding 100% B until 32 min, then decreasing from 100 to 3% B from 32 to 33 min, and finally holding 3% B until 36 min. The flow rate was 0.4 mL/min, the injection volume was 5 µL, and the column temperature was maintained at 35 °C.

Mass spectrometry data were acquired over an m/z range of 50–1200 in both positive and negative electrospray ionization (ESI) modes, using the following parameters: gas flow of 9 L/min, nebulizer pressure at 38 psi, dry gas flow of 9 L/min, and a dry temperature of 220 °C. The capillary and end plate offset voltages were adjusted to 4500 V and 500 V, respectively. External calibration of the instrument was performed using a 1 mM sodium formate/acetate solution in isopropanol/water (50/50) with 0.2% formic acid, directly infused into the source.

To ensure system stability, three consecutive injections of chloramphenicol (ESI– mode; $\Delta RT = 0.02$ min; $\Delta m/z = 0.002$) and triphenyl phosphate (ESI + mode; $\Delta RT = 0.02$ min; $\Delta m/z = 0.001$) were carried out before sample injections. Calibration solution injections were performed at the beginning of each run, and all spectra were recalibrated before statistical analysis.

MS/MS fragmentation was carried out based on the accurate mass and retention time (RT) previously determined, using different collision energy ramps ranging from 15 to 50 eV to induce fragmentation. Peak alignment and detection were carried out using the T–Rex 3D algorithm in the MetaboScape 4.0 software (Bruker Daltonics, Billerica, MA, USA).

Tentative compound identification was performed based on accurate mass metabolites listed in various publicly accessible databases, including METLIN, KEGG, Pubchem, HMDB, and the Plant Metabolic Network. Furthermore, partial structural identification of key metabolites was further refined by comparing their MS/MS fragmentation patterns with those of reference compounds available in the aforementioned databases.

Statistical analysis

Statistical analyses were performed using Statistix 8.0 software. Data normality and homoscedasticity were assessed using the Shapiro–Wilk test ($P \leq 0.05$). A Student's t-test was used to compare means (lesions area and GSLs content), with statistically significant differences indicated by a single asterisk ($P \leq 0.05$). One-way ANOVA using Tukey's multiple range test was used for pairwise comparisons (enzymatic activity, and oligomers quantity); different letters indicate significant differences ($P \leq 0.05$).

Statistical analysis of the metabolomic data was conducted using the online platform Metaboanalyst (Chong et al. 2019). To eliminate non-informative variables, the interquartile range (IQR) filter was applied. Additionally, Pareto variance scaling was utilized to adjust for offsets and to equalize the significance of both high- and low-abundance ions. The resulting three-dimensional matrix (comprising peak indices, samples and variables) was subjected to further statistical evaluation. A two-sample t-test was performed with a FDR value of ≤ 0.05 to identify differentially expressed metabolites. Furthermore, a partial least squares discriminant analysis (PLS-DA) was employed to explore and visualize the pattern of metabolite variation among treatments. The PLS-DA model was assessed via cross-validation, using R^2 and Q^2 metrics, which estimate the model's explanatory

power and predictive accuracy, respectively. For each treatment comparison, features with a variable importance in projection (VIP) score > 2 in the PLS-DA model were selected and considered the most influential features. Finally, features with a VIP score > 2 and a FDR value threshold < 0.05 were retained.

Results

Elicitor release by *T. hamatum*

Chitinase and β-glucanase enzymatic activities were assessed in the different filtrates obtained from liquid fermentation (Fig. 1). Chitinase activity was detected exclusively in the cultures where *T. hamatum* was present. Of these, cultures in which *T. hamatum* was grown in the presence of chitin or *S. sclerotiorum* mycelium reported the significantly higher chitobiosidase activity (9.6 and 8.3 units/mL, respectively), β-N-acetylglucosaminidase (8.4 and 7.6 units/mL, respectively) and endochitinase (6.6 and 7.8 units/mL, respectively), compared to the other *T. hamatum* filtrates (chitobiosidase: 2.4–4.9 units/mL; β-N-acetylglucosaminidase: 2.7–5.4 units/mL; endochitinase: 1.1–3.4 units/mL) (Fig. 1a).

β-Glucanase activity was quantified in all culture filtrates containing either *T. hamatum* or *S. sclerotiorum*. However, in the case of *S. sclerotiorum* alone, no significant differences were observed compared to control filtrates without fungal presence. All cultures with *T. hamatum* reported β-glucanase activity, being significantly higher than that of the *T. hamatum* culture on *S. sclerotiorum* mycelium (3.5 units/mL),

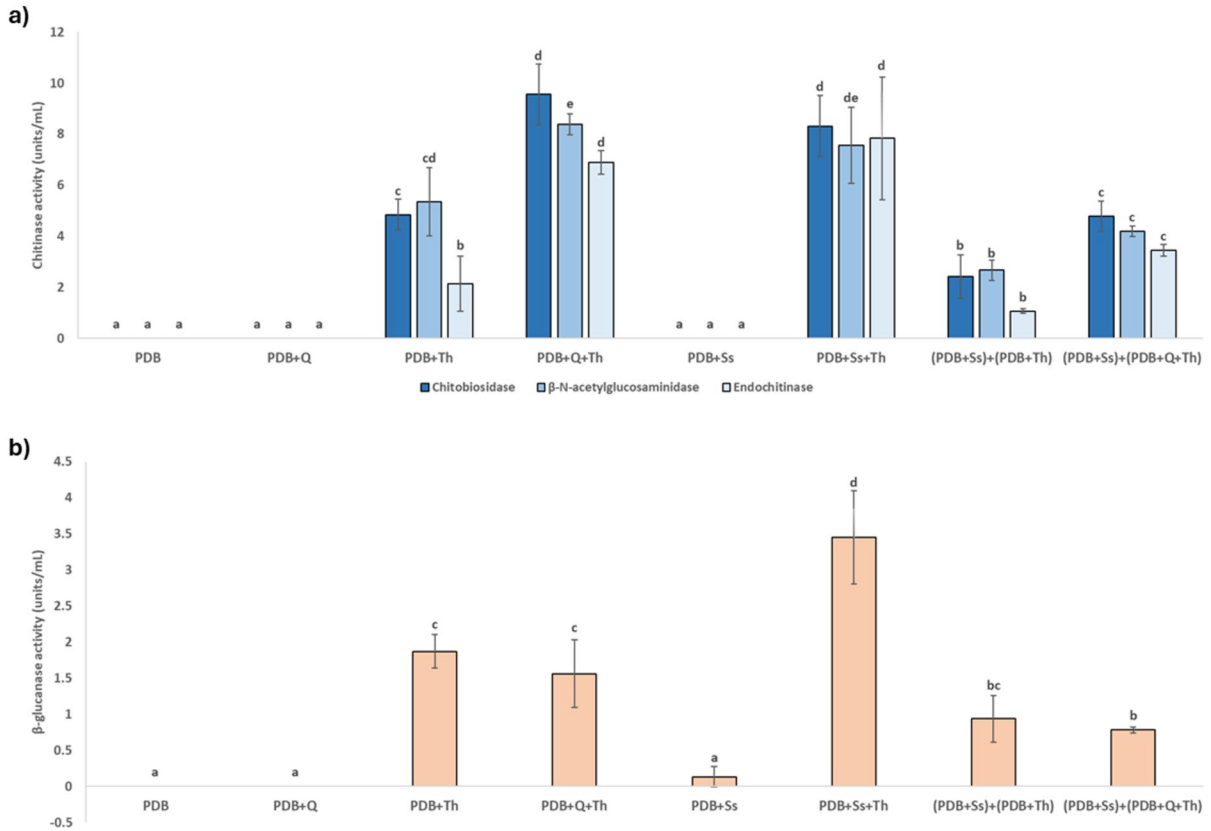

Fig. 1 Chitinase (**a**) and β-glucanase (**b**) activity of different fungal filtrates. Endochitinase and exochitinase (chitobiosidase and β-N-acetylglucosaminidase) activities were analyzed (**a**). PDB: culture medium; Q: chitin; T: *Trichoderma*; Ss: *S. sclerotiorum*. Data are the mean of 30 measurements (10 filtered in triplicate) with the corresponding standard deviation. Tukey's test was performed between filtrates; different letters represent significant differences ($P \leq 0.05$). Information on each of the treatments can be found in Table 1

compared to *T. hamatum* growing alone (1.9 units/mL) or in contact with chitin (1.6 units/mL) (Fig. 1b).

On the other hand, the chitin and glucan oligomers present in these filtrates were quantified (Fig. 2). With respect to chitin oligomers, only cultures with *T. hamatum* and chitin or *T. hamatum* and *S. sclerotiorum* mycelium reported significant differences (0.6–0.8 glucosamine g/L) compared to the rest of the filtrates (Fig. 2a). In contrast, for β-glucan quantification, only the culture of *T. hamatum* grown on *S. sclerotiorum* mycelium showed a significant increase (44 mg/L) compared to all other filtrates (Fig. 2b).

Lesions produced by *S. sclerotiorum* on broccoli leaves

After the application of the different fungal filtrates on plant roots, the possible activation of systemic defenses by foliar infection with *S. sclerotiorum* was determined (Fig. 3). Only the treatment of plants with the fungal filtrates obtained from the interaction between *T. hamatum* and *S. sclerotiorum* mycelium (PDB + Ss + Th treatment) significantly reduced the area of foliar lesions caused by the pathogen (0.76 mm^2), compared to the control treatment (PDB treatment) (1.81 mm^2). The treatment with the filtrates obtained from *T. hamatum* grown alone led to a significant increase in the lesions area (2.92 mm^2), compared to the control. No significant differences were observed in the other treatments when compared to the control (Fig. 3b).

Hormonal plant defense response

To elucidate the potential biochemical mechanisms involved in the activation of systemic defenses in

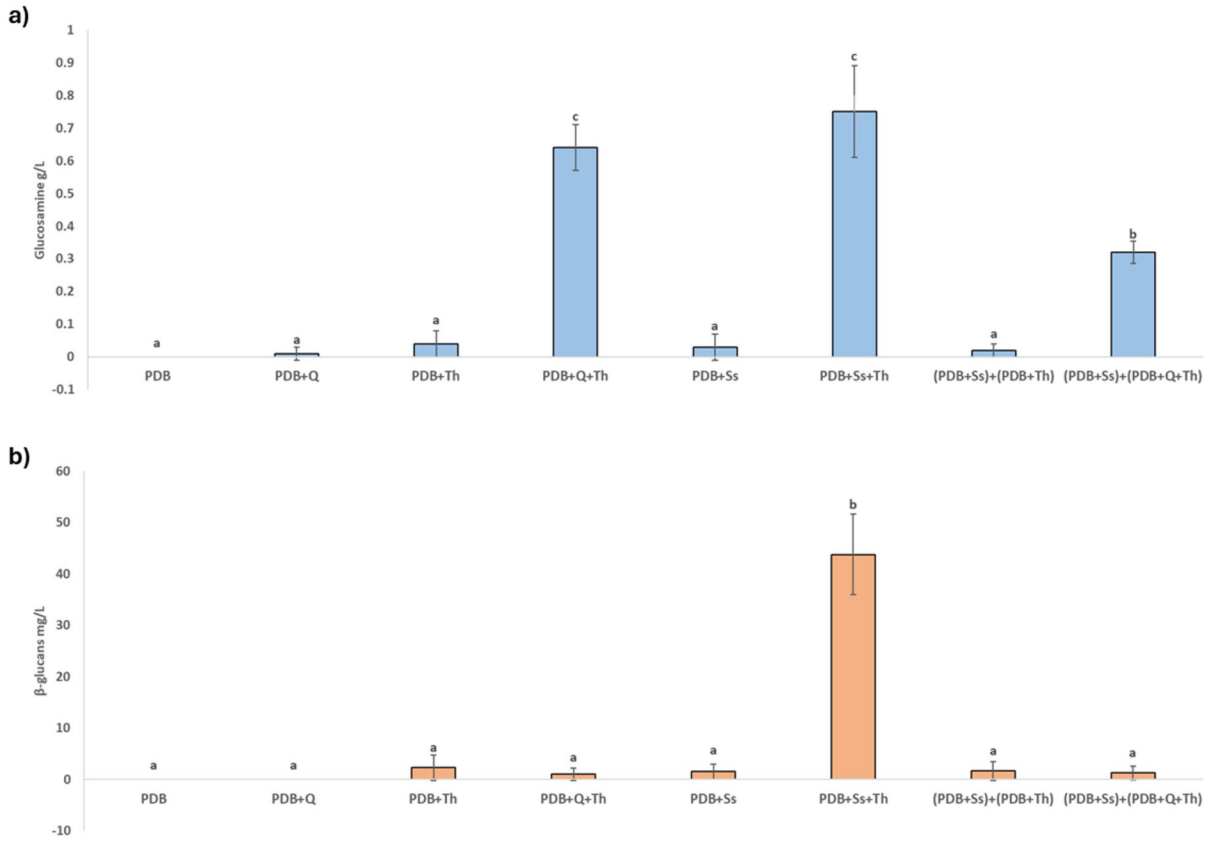

Fig. 2 Glucosamine (**a**) and β-glucans (**b**) quantified on different fungal filtrates. PDB: culture medium; Q: chitin; T: *Trichoderma*; Ss: *S. sclerotiorum*. Data are the mean of 30 measurements (10 filtered in triplicate) with the corresponding standard deviation. Tukey's test was performed between filtrates; different letters represent significant differences ($P \leq 0.05$). Information on each of the treatments can be found in Table 1

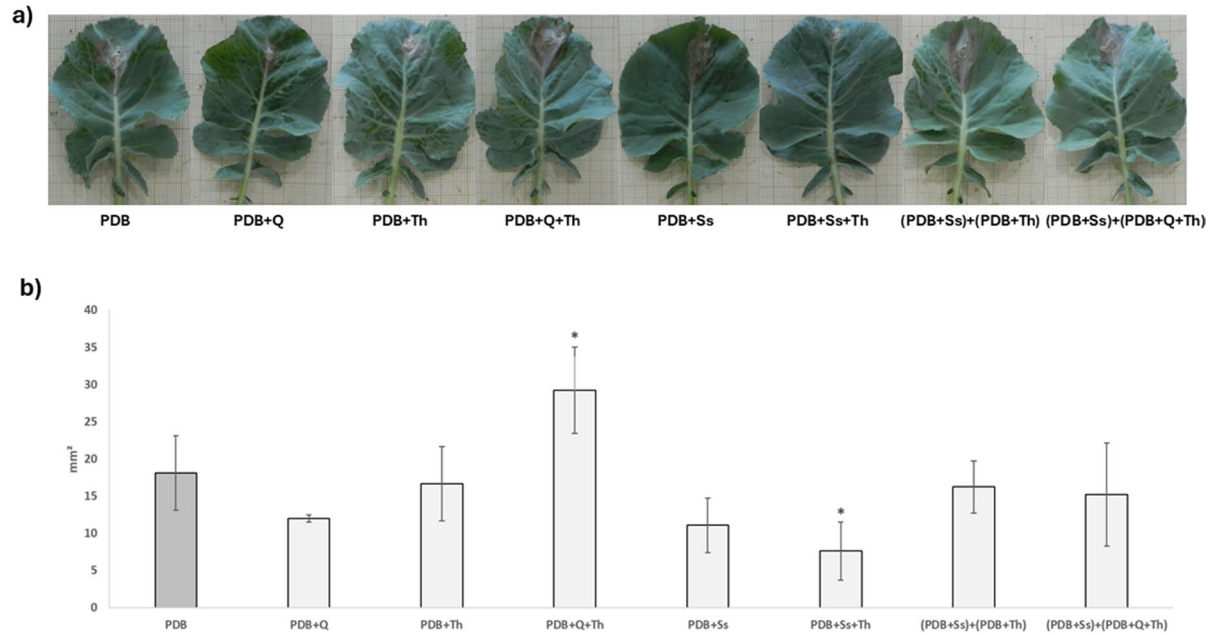

Fig. 3 Lesions caused in broccoli leaves by *S. sclerotiorum* (**a**) and quantification of lesion area (mm^2) (**b**). PDB: culture medium; Q: chitin; T: *Trichoderma*; Ss: *S. sclerotiorum*. Data are the mean of 15 leaves for each condition, with the corresponding standard deviation. One-way analysis of variance (ANOVA) was performed, followed by Student's t-test. The asterisk indicates significant differences between the different treatments and the PDB control treatment ($P \leq 0.05$). Information on each of the treatments can be found in Table 1. The scale black bars on leave-pictures represent 1 cm in length

broccoli plants against *S. sclerotiorum* after root application of the different fungal filtrates, a hormone, GSLs profile and non-target metabolomic study was performed on the aerial part and infected leaves. Hormone analysis reported no significant differences in the levels of gibberellins (GAs), cytokinin (trans-zeatin [tZ] and zeatin riboside [ZR]), auxins (indole-3-acetic acid [IAA], 2-oxindole-3-acetic acid [OxIAA], indole-3-acetyl-aspartate [IAA-Asp] and indole-3-acetyl alanine [IAA-Ala]), ethylene (ET), salicylic acid (SA) and abscisic acid (ABA), among plants root inoculated with PDB compared to the filtrates from the growth of *T. hamatum* on *S. sclerotiorum* mycelium (Table 2). Among growth-related hormones, a significant increase in systemic accumulation of the cytokinin isopentenyladenine (iP) was recorded in plants treated with *T. hamatum* filtrates growing on the pathogen (888.12 ng/g), compared to treatment with PDB filtrates (248.37 ng/g). With respect to stress-related hormones, significant differences were reported in the accumulation of jasmonic acid (JA), with higher accumulation in plants treated with *T. hamatum* filtrates growing on the mycelium of the pathogen and PDB (990.32 ng/g), compared to PDB filtrates (827.78 ng/g). Furthermore, although no significant differences were reported ($P = 0.057$) the mean ET content in plants treated with the different filtrates was distant (694.57 ng/g for PDB filtrates, and 1931.49 ng/g for filtrates from *T. hamatum* growing on *S. sclerotiorum*) (Table 2).

Metabolomic plant defense response

GSLs profiling was conducted in broccoli leaves infected with *S. sclerotiorum*. No significant differences were reported between plants treated with the PDB filtrates, compared to the filtrate of *T. hamatum* growing on *S. sclerotiorum* mycelium, with respect to the total and specific aliphatic GSLs glucoiberin (GIB) and glucotrophanin (GRA), nor the specific indole GSLs 4-methoxyglucobrassicin and neoglucobrassicin (Fig. 4). However, plants treated with *T. hamatum* filtrate growing on the mycelium of the pathogen accumulated significantly higher levels of total GSLs (3.85 and 2.57 nm/mg, respectively), total indole GSLs (2.32 and 1.5 nm/mg, respectively) and

Table 2 Hormone content (ng/g) in broccoli plants, infected with *S. sclerotiorum* (Ss) and root inoculated with PDB and PDB + Ss + Th filtrates (information on each of the treatments can be found in Table 1)

	STRESS HORMONES				CYTOKININS			GIBBERELLINS			AUXINS			
TREATMENT	ET[+]	JA	SA	ABA	tZ	ZR	iP	GA1	GA3	GA4	IAA	OxIAA	IAAAsp	IAAAla
PDB	694.57±458.49	827.78±53.98	1741.63±569.73	39.33±9.82	3442.66±581.68	1699.22±1043.15	248.37±162.64	4.36±2.74	0.47±0.46	1.65±0.88	111.66±21.45	96.73±26.88	117.65±24.94	30.32±0.77
PDB+Ss+Th	1931.49±838.79	990.32±101.25*	1925.06±963.62	40.36±4.99	3703.68±301.23	583.97±169.45	888.12±298.29*	6.39±1.58	0.97±0.76	1.51±0.47	109.45±14.24	116.76±15.51	88.23±40.34	40.29±18.41

[+]Quantified as its precursor 1-aminocyclopropane-1-carboxylate (ACC)

ET: ethylene; JA: jasmonic acid; SA: salicylic acid; ABA: abscisic acid; tZ: trans-zeatin; ZR: zeatin riboside; iP: isopentenyladenine; GA: gibberellic acid; IAA: indole-3-acetic acid; OxIAA: 2-oxindole-3-acetic acid; IAAAsp: indole-3-acetylaspartate; IAAAla: indole-3-acetyl alanine.

Data are the mean of five pools of three broccoli plants with the corresponding SE. The asterisk indicates significant differences between the treatments ($P \leq 0.05$).

specific glucobrassicin (GBS) (1.47 and 0.69 nm/mg, respectively), compared to plants treated with PDB filtrates (Fig. 4).

The data acquired in both ion modes were analyzed using multivariate statistical methods compare the metabolomic profiles of plants treated with either PDB or PDB + Ss + Th. The PLS-DA score plots demonstrated clear discrimination between the two groups, with the first 2 components accounting for over 50% of the total variance (Fig. 5). Generally, the PLS-DA model is considered robust when $Q^2 > 0.5$ and $R^2 > Q^2$ is obtained after an appropriate cross-validation. In this analysis, a $Q^2 > 0.84$ and $R^2 > 0.93$ were obtained, indicating good predictive power. These results indicate that the metabolic profiles of PDB and PDB + Ss + Th are distinct. Therefore, the VIP list with features higher than 2 were used to select the compounds potentially involved in the response to infection. A total of 90 compounds had VIP scores above this threshold, being the main responsible for the groups separation. Of these, 37 features were found at higher concentration in plants treated with the *T. hamatum* filtrate growing on *S. sclerotiorum* mycelium.

When possible, a molecular formula was assigned to each of these 37 metabolites based on the exact mass and the isotopic pattern. Tentative compound identification was performed based on the molecular formula and MS/MS fragmentation pattern. Based on this approach, we were able to putatively assign compound names to 24 out of 37 metabolites (Table 3). The main group of metabolites identified were lipids and derivatives, such as glycerophospholipids (lyso PC 16:0, 17:0, 17:0, 18:0, 18:1, 18:2, 18:3, and lysoPE 16:0, 18: 2), glycerolipids (MG 18:3), saturated fatty acids (13S-hydroxy-11E-octadec-9-ynoic acid) or alkyl glyceryl ethers (1-O-(2R-hydroxy-hexadecyl)-sn-glycerol). Different alkylamides (N-(2-hydroxyethyl)henicosa-9,12,15-trienamide and N-(2-hydroxyethyl)nonadeca-6,9,12-trienamide) and fattyamides (palmitoylcholine and linoleoylcholine) were also identified, together with GSLs (GBS), vitamins (niacin) and chlorophyll precursors or derivatives (pheophorbide A, 7-hydroxychlorophyllide and red chlorophyll catabolite) (Table 3).

Discussion

Although *Trichoderma* species are well known for their ability to activate both systemic and local plant

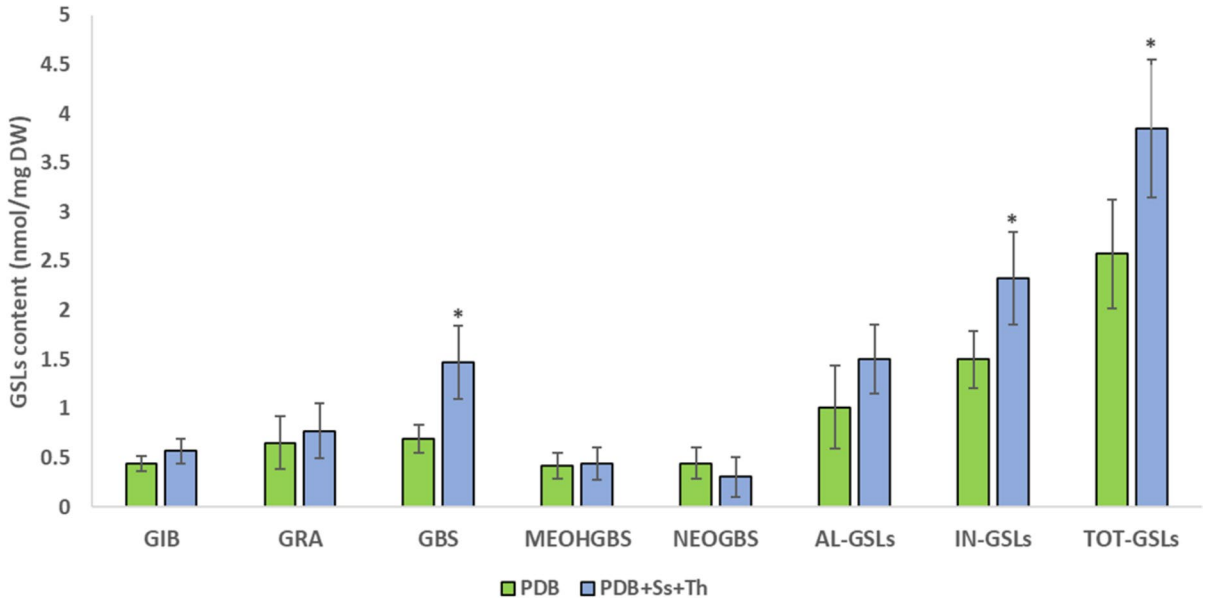

Fig. 4 Mean of individual GSL content detected in broccoli leaves: glucoiberin (GIB), glucoraphanin (GRA), glucobrassicin (GBS), 4-methoxyglucobrassicin (MEOHGBS), neoglucobrassicin (NEOGBS), and mean of grouped aliphatic (AL-GSL), indole (IN-GSL) and total (Tot-GSL) glucosinolate content in broccoli leaves collected from conventional (CONV) and organic (ORG) fields. PDB: culture medium; Th: *Trichoderma*; Ss: *S. sclerotiorum*. Data are the mean of 15 leaves for each condition, with the corresponding standard deviation. One-way analysis of variance (ANOVA) was performed, followed by Student's t-test. The asterisk indicates significant differences between the treatments PDB and PDB + Ss + Th ($P \leq 0.05$). Information on each of the treatments can be found in Table 1

defense responses through colonization of the root apoplast (Khan et al. 2023), other possible indirect mechanisms by interacting with pathogens could be involved in its defense-inducing capacity in plants. The working hypothesis of this study was that *T. hamatum* could release oligomers from the cell wall of the pathogen *S. sclerotiorum*, which could act as elicitors of plant defense responses. These oligomers would likely include fragments of chitin and/or glucans, the main structural components of the *S. sclerotiorum* cell wall (Liu and Free 2016).

After *T. hamatum* was grown in contact with *S. sclerotiorum* mycelium was reported an increase in chitinase and β-glucanase enzyme activity by *Trichoderma*, along with the release of glucosamine and β-glucan oligomers into the liquid culture medium. Both chitinase activity and release of glucosamine oligomers were also reported when growing *T. hamatum* on commercial chitin. However, only fungal filtrates from *T. hamatum* grown on *S. sclerotiorum* were able to effectively induce systemic defenses against foliar infection by the pathogen. These results suggest that the β-glucans released from the *S. sclerotiorum* cell wall by *T. hamatum* β-glucanases could act as elicitors of plant systemic defenses, unlike glucosamines released by chitinase activity. In this sense, the β-glucans derived from the fungal cell walls have been previously described as effective elicitors of systemic defensive defenses (Perrot et al. 2022; Riseh et al. 2023), as have glucosamines (Chaliha et al. 2018, 2020).

Although it would be expected that filtering the culture medium of *Trichoderma* with commercial chitin would induce systemic defenses in plants, given that it is rich in chitin oligomers, no significant differences were observed compared to control plants. Further research is needed to elucidate the molecular and physiological mechanisms underlying this lack of systemic defense activation. It is also noteworthy that treatment with filtrates obtained from *T. hamatum* growing on PDB caused significantly greater leaf damage by the pathogen. This effect may be explained by the recognition of *Trichoderma* filtrates by the roots, leading to the

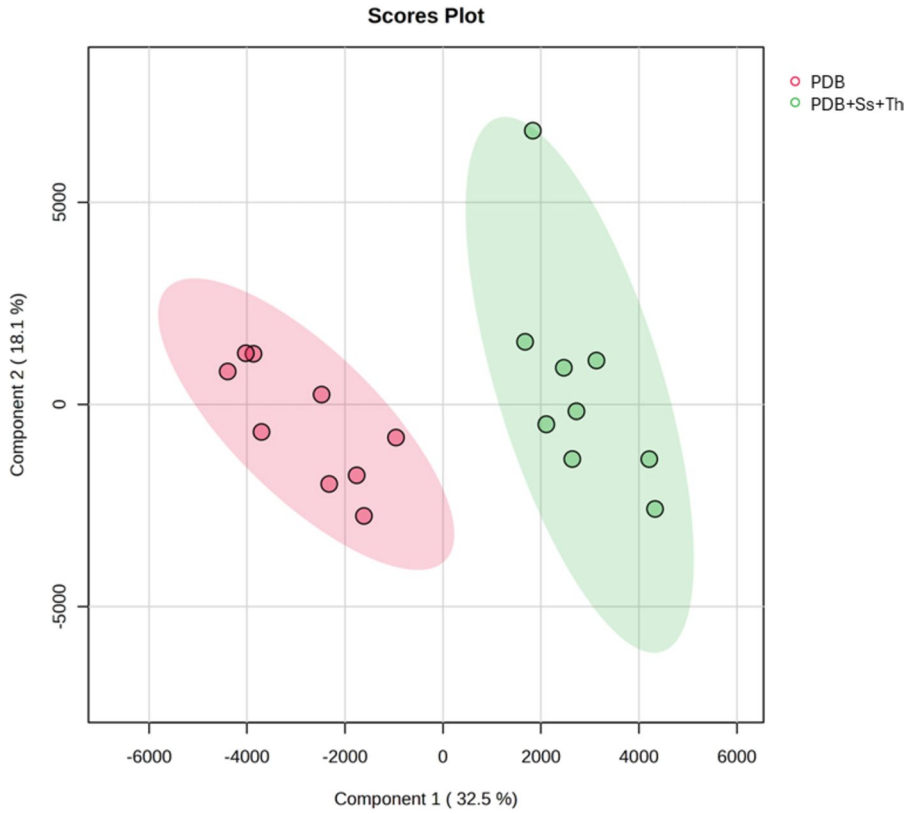

Fig. 5 Score-plot of the two principal components from a PLS-DA analysis of untargeted metabolomics. The two treatments used in the analysis were PDB and PDB + Ss + Th. Information on each of the treatments can be found in Table 1. PDB: culture medium; Th: *Trichoderma*; Ss: *S. sclerotiorum*. Fifteen biological replicates (leaves) were analyzed per treatment

activation of localized root defenses at the expense of systemic responses. It is possible that the enhancement of root defenses in response to *Trichoderma* exposure redirects the plant's defensive resources, thereby impairing the systemic activation of defenses against foliar pathogens. However, an in-depth study is required to discern the mechanism involved in the lack of activation of systemic defenses in the specific case of *T. hamatum* filtrates.

The main CWDEs that *Trichoderma* uses in mycoparasitism are chitinases. Although β-glucanases have been suggested to play fundamental roles in specific fungal interactions, their contribution to mycoparasitism is often considered redundant (Mukherjee et al. 2022). However, in the specific case of *Trichoderma* mycoparasitism against *S. sclerotiorum*, β-glucanases have been reported to play a key role in this mechanism of action, both on the mycelium (Troian et al. 2014) and sclerotia (Geraldine et al. 2013) of the pathogen. Therefore, *T. hamatum* could release β-glucan oligomers through its mycoparasitic activity, which would act as root elicitors of systemic plant defenses. Nonetheless, this mechanism of action may not be relevant in interactions with other pathogens where *Trichoderma* does not rely on β-glucanase production for its antagonistic action.

Both glucans and glucosamines have been widely described as effective elicitors of plant defenses (Guarnizo et al. 2020; Poveda and Díez-Méndez 2023). However, glucosamine-rich fungal filtrates obtained from *T. hamatum* growth on commercial chitin did not enhance the systemic plant defense response against foliar infections caused by *S. sclerotiorum*. In contrast, only fungal filtrates rich in glucans (44 mg/L) and glucosamines (0.8 g/L), derived from *T. hamatum* grown on *S. sclerotiorum* mycelium, were able to reduce systemic infection. These results suggest that only glucans released from the pathogen's cell wall by *T. hamatum* could act as effective elicitors.

In the treatments carried out, we used live pathogen filtrates (PDB + Ss) as a control to detect the possible effects that compounds produced by *S. sclerotiorum* may have on the activation of plant defenses. However, when studying the effect of elicitors possibly released from the pathogen's cell wall by

Table 3 Tentative identification of major metabolites with a |log2 (*FC*)|≥ 1 in plants treated with PDB + Ss + Th compared with plants treated with PDB. Metabolites are sorted by ionization mode

Mass	*P* value	VIP score	Rt (sec)	Ionization	mz	Formula	MSMS	Putative name
592.26886	0.0477	9.3931	1798.17	M + H	593.2761	$C_{35}H_{36}N_4O_5$	533.251, 565.276, 575.261	Pheophorbide A
495.33139	0.0244	7.2851	1499.34	M + H	496.3399	$C_{24}H_{50}NO_7P$	184.073, 104.106, 86.096, 124.999, 478.326	LysoPC(16:0)
363.31401	0.0303	6.2917	1392.6	M + H	364.3213	$C_{23}H_{41}NO_2$	305.245, 55.054, 67.054, 81.069, 93.069, 95.09	(9Z,12Z,15Z)-N-(2-hydroxyethyl)henicosa-9,12,15-trienamide
517.31694	0.0390	6.1904	1420.43	M + H	518.3243	$C_{26}H_{48}NO_7P$	184.073, 104.106, 86.096, 124.999	LysoPC(18:3(9Z,12Z,15Z))
519.33287	0.0367	5.0311	1463.42	M + H	520.34	$C_{26}H_{50}NO_7P$	184.073, 104.107, 86.096, 337.273	LysoPC(18:2(9Z,12Z))
453.28606	0.0329	4.2181	1486.5	M + H	454.293	$C_{21}H_{44}NO_7P$	313.272, 282.272, 62.06, 57.071, 71.085	LysoPE(16:0/0:0)
453.28606	0.0330	3.0324	1412.44	M + Na	476.2774	$C_{21}H_{44}NO_7P$	335.257, 304.262, 62.061, 95.085, 81.07	LysoPE(16:0/0:0)
608.26372	0.0236	3.5917	1746.02	M + H	609.2708	$C_{35}H_{36}N_4O_6$	591.256, 531.236, 559.23, 550.253	7-hydroxychlorophyllide a
335.28265	0.0127	3.5458	1343.78	M + H	336.2899	$C_{21}H_{37}NO_2$	277.214, 67.053, 79.053, 93.069, 99.043	(6Z,9Z,12Z)-N-(2-hydroxyethyl)nonadeca-6,9,12-trienamide
341.32972	0.0530	3.4954	1443.82	M + H	342.337	$C_{21}H_{43}NO_2$	283.261, 57.07	Palmitoylcholine
608.2633	0.0044	3.4418	1726.61	M + H	609.2706	$C_{34}H_{40}O_{10}$	591.256, 531.236, 559.23, 550.253	-
521.34861	0.0088	3.2206	1518.93	M + H	522.3556	$C_{26}H_{52}N_{O7}P$	184.072, 104.106, 86.096, 504.34	LysoPC(18:1(11Z))
146.03674	0.0010	3.0918	628.2	M + H	147.044	$C_9H_6O_2$	-	-
196.11008	0.0010	3..356	925.96	M + H	197.1175	$C_{11}H_{16}O_3$	91.054, 105.07, 133.1, 67.054, 79.054	-

Table 3 (continued)

Mass	*P* value	VIP score	Rt (sec)	Ionization	mz	Formula	MSMS	Putative name
352.26114	0.0060	3.0202	1402.93	M + H	353.2688	$C_{21}H_{36}O_4$	67.504, 79.503, 81.07, 95.085, 107.085, 121.1	MG(18:3(9Z,12Z,15Z)/0:0/0:0
500.15315	0.2132	3.0085	1123.8	M + H	501.1604	$C_{22}H_{28}O_{13}$	177.054, 85.028, 127.039, 145.028, 195.065	-
137.04788	0.0010	2.9171	60.53	M + H	138.0552	$C_7H_7NO_2$	-	-
523.36404	0.0078	2.8683	1599.96	M + H	524.3714	$C_{26}H_{54}NO_7P$	184.072, 104.106, 86.196, 506.358	LysoPC(18:0)
541.33768	0.0258	2.8155	1499.04	M-H	540.3304	$C_{25}H_{52}NO_9P$	-	-
784.47347	0.0706	2.7732	1711.96	M + H	785.4807	$C_{45}H_{68}O_{11}$	507.252, 184.072, 519.288, 491.257	-
812.50483	0.0223	2.7635	1766.82	M + H	813.5121	$C_{42}H_{72}N_2O_{13}$	519.292, 535.286, 335.257	-
477.28642	0.0010	2.7614	1453.28	M + H	478.2933	$C_{23}H_{44}NO_7P$	337.271, 62.06, 95.085, 81.069, 306.277	LysoPE(18:2(9Z,12Z)/0:0)
509.34877	0.0349	2.7372	1530.07	M + H	510.3556	$C_{25}H_{52}NO_7P$	184.072, 104.106, 86.095	LysoPC(17:0)
563.32198	0.0010	2.4627	1420.39	M-H	562.3147	$C_{25}H_{41}N_9O_6$	-	-
365.32954	0.0358	2.3671	1421.38	M + H	366.3368	$C_{23}H_{43}NO_2$	307.261, 55.054, 67.054, 69.061, 81.065, 95.09	Linoleoylcholine
495.33312	0.0246	2.3489	1483.97	M + H	496.3401	$C_{25}H_{46}N_5O_3P$	184.072, 104.106, 86.096, 124.999	LysoPC(16:0)
722.37192	0.0119	2.3089	1403.03	M-H	721.3646	$C_{34}H_{58}O_6$	397.136, 277.218, 415.146, 119.035, 89.025	-
448.06082	0.0010	2.2762	544.21	M-H	447.0535	$C_{16}H_{20}N_2O_9S_2$	96.961, 74.992, 259.015, 195.036	Glucobrassicin
122.04758	0.0011	2.2591	90.46	M + H	123.0549	$C_6H_6N_2O$	80.049, 53.039, 78.033, 96.044	Niacin
517.31719	0.0390	2.1881	1408.91	M + Na	540.304	$C_{26}H_{48}NO_7P$	481.23, 104.107, 146.982, 335.259	LysoPC(18:3(9Z,12Z,15Z))

Table 3 (continued)

Mass	*P* value	VIP score	Rt (sec)	Ionization	mz	Formula	MSMS	Putative name
352.26147	0.0010	2.1799	1472.25	M + H	353.2689	$C_{21}H_{36}O_4$	67.054, 81.07, 95.085, 107.085, 297.277	MG(18:3(9Z,12Z,15Z)/0:0/0:0)
626.27421	0.0089	2.1522	1458.12	M + H	627.2815	C35H38N4O7	567.259, 545.401	red chlorophyll catabolite(2 −)
624.2623	0.0216	2.1369	1730.94	M + H	625.2696	$C_{38}H_{41}O_6P$	-	-
294.21961	0.0109	2.1224	1548.74	M + Na	317.2087	$C_{18}H_{30}O_3$	62.06, 67.053, 81.069, 93.069, 107.085	13S-hydroxy-11E-octadec-9-ynoic acid
565.33719	0.0349	2.0844	1463.45	M-H	564.3299	$C_{27}H_{52}NO_9P$	-	-
332.29275	0.0005	2.0615	1689.15	M + Na	355.282	$C_{19}H_{40}O_4$	57.07, 69.069, 83.085, 97.101, 111.116	1-O-(2R-hydroxy-hexadecyl)-sn-glycerol
532.28818	0.0010	2.0476	1399.06	M-H	531.2809	$C_{26}H_{44}O_{11}$	249.186, 44.998, 161.046	-

Trichoderma in this work, we grew *T. hamatum* on autoclaved *S. sclerotiorum* mycelium (PDB + Ss + Th treatment). The autoclaving of the pathogen mycelium itself could cause the release of elicitors (such as glucans and glucosamines). For this reason, after autoclaving the mycelium, it was washed to remove possible elicitors and/or compounds released by the *S. sclerotiorum* mycelium during autoclaving. This procedure allows us to eliminate from the study the possible effect produced by these potential elicitors released by autoclaving. In this regard, future studies should characterize the possible compounds and molecules released from the cell walls of *S. sclerotiorum* during the autoclaving of its mycelium.

It is important to emphasize that, beyond the quantitative analyses of enzyme activity (chitinases and β-glucanases) and the oligomers detected, other unidentified molecules with potential elicitor activity may also be present. These could include additional oligomers as well as fungal secondary metabolites. The fungal cell wall is mainly composed of glucans and chitin, however, other fungal oligomers could be released in our assays and could contribute to the activation of plant defenses (Ruiz-Herrera and Ortiz-Castellanos 2019). Future work involving the isolation and characterization of specific oligomers are needed to determine the specificity of these fungal compounds in triggering plant defense responses, as well as to elucidate the molecular mechanisms underlying fungal recognition by the plant.

In order to determine the mechanisms involved in the systemic defenses activated by *S. sclerotiorum* cell wall oligomers, a multi-omics approach was employed, including hormone profiling, GSL analysis and non-targeted metabolomics. Hormonomic analysis reported that root recognition of these oligomers by broccoli plants induced a systemic accumulation of JA, iP and ET hormones. JA and ET mediate plant defensive responses against necrotrophic pathogens (Macioszek et al. 2023), such as *S. sclerotiorum* (Poveda et al. 2023). On the other hand, iP has been described as a hormone involved in the activation of systemic plant defenses against biotrophic/hemibiotrophic pathogens (Hönig et al. 2023; Liang et al. 2024). Therefore, these findings suggest that pathogen oligomers released by *T. hamatum* would induce the activation of systemic plant defenses against necrotrophic and biotrophic/hemibiotrophic pathogens, although no significant differences were reported with respect to systemic SA accumulation. Nevertheless, fungal secondary metabolites released by *S. sclerotiorum* when attacked by *Trichoderma* could also be acting as elicitors of plant systemic hormones signal, an aspect that needs further study.

The reduced *S. sclerotiorum* infection observed on broccoli leaves following root treatment with pathogen-derived oligomers was associated with increased accumulation of the GSL GBS. This metabolite has been widely described as a potent antifungal against several necrotrophic fungi (Saharan et al. 2021; Aghajanzadeh et al. 2023; Rodriguez et al., 2023), including *S. sclerotiorum* (Teng et al. 2021a, 2021b).

Along with this GSL, non-targeted metabolomics analysis identified other metabolites differentially accumulated in leaves that were more resistant to the pathogen, following root inoculation with the oligomers. Among them, niacin was detected, a compound previously reported to possess antifungal against necrotrophic pathogens, such as *Botrytis cinerea* (Hong et al. 2016) or *Sclerospora graminicola* (Pushpalatha et al. 2007). However, its antifungal effect against *S. sclerotiorum* has not been previously described, making this study a potential first report in that context. Further research using the isolated metabolite is required to confirm its antimicrobial properties against this pathogen. In addition, several fatty acids were identified that may contribute to the enhanced defensive capacity observed in plants exposed to *S. sclerotiorum*. A wide variety of fatty acids have been described as signal molecules in the activation of plant defenses against pathogens (Kachroo et al., 2009; Lim et al. 2017). Specifically, various fatty acids have been described as signal molecules involved in the defense of cruciferous plants, such as *Brassica napus*, against foliar infection by *S. sclerotiorum* (Liu et al. 2022). The remaining metabolites identified in leaves with reduced pathogen infection would not be related to effective systemic resistance against *S. sclerotiorum*, as they have not yet been reported as antifungal and/or plant defense-related compounds. However, future studies involving individual metabolites are needed to confirm the absence of antifungal activity.

Therefore, this work proposes a possible novel mechanism of action that complements the well-established modes of *Trichoderma*. This novel mechanism would involve the co-action of two already known mechanisms: mycoparasitism and the induction of plant defenses. Through the lytic action of the mycoparasitic CWDEs, *Trichoderma* would release oligomers, specifically glucans, from the cell wall of the pathogenic fungus. These oligomers could then be recognized by root cells as elicitors, triggering the induction of systemic plant defenses.

Study limitations

This study represents the first approach to propose a novel mechanism of action as a BCA developed by *Trichoderma*. Despite the different results reported in the various analyses, both in vitro and *in planta*, there are important aspects that must be addressed in future research to fully understand and validate this possible new mechanism of action.

Once the ability of glucan oligomer filtrates to induce systemic plant defenses has been confirmed, future research should prioritize dose–response studies. Additionally, these studies should be extended to other crops to facilitate the development of commercially viable agricultural formulations based on these potential elicitors.

As discussed above, although fungal culture filtrates enriched in glucan oligomers have been shown to induce systemic plant defenses, these filtrates may also contain many other different molecular components, such as enzymes, metabolites, and/or other oligomers. Future research should aim to directly verify whether glucan oligomers are the primary elicitors responsible for this newly proposed mechanism of action. As a first step, a study should be conducted in which purified oligomers isolated from the filtrates, along with their commercial equivalents, are applied directly to the roots. These oligomers would be derived from both glucans and chitin, to enable a specific comparison of their respective effects on plant defense responses. Moreover, the role of glucan oligomers as elicitors could be validated using *T. hamatum* knock-out mutants deficient in their production. However, this approach may be limited by the essential structural role these polysaccharides play in fungal cell wall integrity and overall viability.

In addition to the molecular approaches already employed, the elicitor effect of glucan oligomers released from the cell walls of the pathogenic fungus should be validated at the molecular level. This aspect could be addressed in future work through a direct study of the activation of PRRs in root cells. In addition, specific molecular responses in these cells, such as the ROS burst, should also be examined.

This study examined the interaction between *T. hamatum* and the pathogen *S. sclerotiorum*. Future research should explore additional interaction combinations, including different *Trichoderma* species and strains, as well as other phytopathogenic fungi.

Furthermore, given that *Trichoderma* also exhibits parasitic activity against oomycetes and the eggs and juveniles of nematodes, these lines of investigation should be extended to encompass these pathogen groups as well.

Finally, this work has yielded additional noteworthy findings that warrant further investigation. Despite the large number of studies confirming *Trichoderma*'s ability to induce systemic plant defenses, *T. hamatum* filtrates grown solely on PDB and applied to the roots caused a "negative effect" on foliar defenses against the pathogen. Future research should focus on the biochemical characterization of these filtrates in order to identify the possible compounds involved in these plant responses. Moreover, it is essential to elucidate the underlying mechanisms within the plant, specifically, which signaling pathways are being activated and inhibited and what happens at the local and systemic levels.

Conclusions

As conclusions, *T. hamatum* could release oligomers from the cell wall of *S. sclerotiorum*, which could be perceived by plant roots and subsequently trigger systemic defense responses. Specifically, glucan oligomers could induce systemic defenses against necrotrophic and/or biotrophic/hemibiotrophic pathogens mediated by JA/ET and or iP. This defense activation is associated with the foliar accumulation of antifungal metabolites, such as GBS and niacin and several fatty acids. Nevertheless, further studies are necessary to rule out the potential elicitor activity of other fungal wall oligomers and/or secondary metabolites.

This study not only proposes a potential new mechanism of action for *Trichoderma*, but also paves the way for the development of novel biofungicides based on cell wall oligomers from phytopathogenic fungi. While further research is necessary to fully explore this emerging area, the identification of specific oligomers capable of triggering plant defense responses could provide the foundation for the formulation of effective commercial products based on these elicitor molecules. The large-scale production of such elicitors may be achieved through fungal fermentation techniques, as demonstrated in this study, by cultivating *Trichoderma* on the mycelium of pathogenic fungi using industrial liquid-phase bioreactors. These novel biofungicides could be readily applied in agricultural settings via existing irrigation and/or fertigation systems.

Author contributions J.P. and P.V. conceived and designed the experiments. J.P., P.V., R.A. and M.D.U. performed the experiments and analysis. J.P. analyzed the data and wrote the manuscript. P.V. contributed to manuscript correction and critical reading. All authors have read and agreed to the published version of the manuscript.

Funding Open access funding provided by FEDER European Funds and the Junta de Castilla y León under the Research and Innovation Strategy for Smart Specialization (RIS3) of Castilla y León 2021-2027. María Díaz-Urbano was funded by the project IN607A 2021/03, Xunta de Galicia, Spain.

Data availability All data supporting the findings of this study are available within the paper.

Declarations

Conflict of interest The authors declare that they have no known competing financial interests or personal relationships that could have influenced the work reported in this paper.

References

Abdul-Malik NA, Kumar IS, Nadarajah K (2020) Elicitor and receptor molecules: orchestrators of plant defense and immunity. Int J Mol Sci 21:963. https://doi.org/10.3390/ijms21030963

Afzal I, Sabir A, Sikandar S (2021) *Trichoderma*: Biodiversity, abundances, and biotechnological applications. In: Yadav AN (ed) Recent Trends in Mycological Research, vol 1. Agricultural and Medical Perspective. Springer, Berlin, Germany, pp 293–315

Aghajanzadeh TA, Watanabe M, Tohge T, Hawkesford MJ, Fernie AR, Hoefgen R et al (2023) Necrotrophic fungal infection affects indolic glucosinolate metabolism in

Brassica rapa. Acta Physiol Plant 45:64. https://doi.org/10.1007/s11738-023-03546-3

Albacete A, Ghanem ME, Martínez-Andújar C, Acosta M, Sánchez-Bravo J, Martínez V et al (2008) Hormonal changes in relation to biomass partitioning and shoot growth impairment in salinized tomato (*Solanum lycopersicum* L.) plants. J Exp Bot 59:4119–4131. https://doi.org/10.1093/jxb/ern251

Almario J, Fabiańska I, Saridis G, Bucher M (2022) Unearthing the plant–microbe quid pro quo in root associations with beneficial fungi. New Phytol 234:1967–1976. https://doi.org/10.1111/nph.18061

Amerio NS, Barengo MP, Bich GA, Castrillo ML (2024) Molecular interactions of *Trichoderma*: from microbial competition to soil health promotion. Int J Mol Biol 7:135–138. https://doi.org/10.15406/ijmboa.2024.07.00183

Brown B, Aaron M (2001) The politics of nature. In: Smith J (ed) The rise of modern genomics, 3rd edn. Wiley, New York, pp 230–257

Chaliha C, Rugen MD, Field RA, Kalita E (2018) Glycans as modulators of plant defense against filamentous pathogens. Front Plant Sci 9:928. https://doi.org/10.3389/fpls.2018.00928

Chaliha C, Field RA, Kalita E (2020) Glycans as plant defense priming agents against filamentous pathogens. In: Mérillon JM, Ramawat KG (eds) Plant Defence: Biological Control. Springer, Berlin, Germany, pp 99–118

Chen RS, Wang JY, Sarwar R, Tan XL (2023) Genetic breakthroughs in the *Brassica napus–Sclerotinia sclerotiorum* interactions. Front Plant Sci 14:1276055. https://doi.org/10.3389/fpls.2023.1276055

Chong J, Wishart DS, Xia J (2019) Using MetaboAnalyst 4.0 for comprehensive and integrative metabolomics data analysis. Curr Protoc Bioinformatics 68:e86. https://doi.org/10.1002/cpbi.86

dos Santos LBPR, Oliveira-Santos N, Fernandes JV, Jaimes-Martinez JC, De Souza JT, Cruz-Magalhães V, Loguercio LL (2022) Tolerance to and alleviation of abiotic stresses in plants mediated by *Trichoderma* spp. In: Amaresan N, Sankaranarayanan A, Dwivedi MK, Druzhinina IS (eds) Advances in *Trichoderma* biology for agricultural applications. Springer, Berlin, Germany, pp 321–359

Dutta P, Mahanta M, Singh SB, Thakuria D, Deb L, Kumari A et al (2023) Molecular interaction between plants and *Trichoderma* species against soil-borne plant pathogens. Front Plant Sci 14:1145715. https://doi.org/10.3389/fpls.2023.1145715

Frolova GM, Berestetskiy AO (2024) Structural diversity of fungal elicitors. Appl Biochem Microbiol 60:1061–1073. https://doi.org/10.1134/S0003683824605973

Geraldine AM, Lopes FAC, Carvalho DDC, Barbosa ET, Rodrigues AR, Brandão RS et al (2013) Cell wall-degrading enzymes and parasitism of sclerotia are key factors on field biocontrol of white mold by *Trichoderma* spp. Biol Control 67:308–316. https://doi.org/10.1016/j.biocontrol.2013.09.013

Guarnizo N, Oliveros D, Murillo-Arango W, Bermúdez-Cardona MB (2020) Oligosaccharides: defense inducers, their recognition in plants, commercial uses and perspectives. Molecules 25:5972. https://doi.org/10.3390/molecules25245972

Gupta N (2020) *Trichoderma* as Biostimulant: Factors responsible for plant growth promotion. In: Manoharachary C, Singh HB, Varma A (eds) *Trichoderma*: Agricultural Applications and Beyond. Springer, Berlin, Germany, pp 287–309

Guzmán-Guzmán P, Kumar A, de Los Santos-Villalobos S, Parra-Cota FI, Orozco-Mosqueda MDC, Fadiji AE et al (2023) *Trichoderma* species: our best fungal allies in the biocontrol of plant diseases—a review. Plants 12:432. https://doi.org/10.3390/plants12030432

Hong JK, Kim HJ, Jung H, Yang HJ, Kim DH, Sung CH et al (2016) Differential control efficacies of vitamin treatments against bacterial wilt and grey mould diseases in tomato plants. Plant Pathol J 32:469. https://doi.org/10.5423/PPJ.OA.03.2016.0076

Hönig M, Roeber VM, Schmülling T, Cortleven A (2023) Chemical priming of plant defense responses to pathogen attacks. Front Plant Sci 14:1146577. https://doi.org/10.3389/fpls.2023.1146577

Hossain MM, Sultana F, Li W, Tran LSP, Mostofa MG (2023) *Sclerotinia sclerotiorum* (Lib.) de Bary: insights into the pathogenomic features of a global pathogen. Cells 12:1063. https://doi.org/10.3390/cells12071063

Kachroo A, Kachroo P (2009) Fatty acid–derived signals in plant defense. Annual Review of Phytopathology 47: 153–176. https://doi.org/10.1146/annurev-phyto-080508-081820

Karlsson M, Atanasova L, Jensen DF, Zeilinger S (2017) Necrotrophic mycoparasites and their genomes. Microbiol Spectr 5:10–1128. https://doi.org/10.1128/microbiolspec.funk-0016-2016

Katano H, Takakuwa M, Hayakawa H, Kimoto H (2016) Determination of chitin based on the colorimetric assay of glucosamine in acidic hydrolysate. Anal Sci 32:701–703. https://doi.org/10.2116/analsci.32.701

Khan RAA, Najeeb S, Chen J, Wang R, Zhang J, Hou J, Liu T (2023) Insights into the molecular mechanism of *Trichoderma* stimulating plant growth and immunity against phytopathogens. Physiol Plant 175:e14133. https://doi.org/10.1111/ppl.14133

Kubiak A, Wolna-Maruwka A, Pilarska AA, Niewiadomska A, Piotrowska-Cyplik A (2023) Fungi of the *Trichoderma* genus: future perspectives of benefits in sustainable agriculture. Appl Sci 13:6434. https://doi.org/10.3390/app13116434

Kupetz M, Aumer J, Harms D, Zarnkow M, Sacher B, Becker T (2017) High-throughput β-glucan analyses and their relationship with beer filterability. Eur Food Res Technol 243:341–351. https://doi.org/10.1007/s00217-016-2748-3

Lana M, Simón O, Velasco P, Rodríguez VM, Caballero P, Poveda J (2023) First study on the root endophytic fungus *Trichoderma hamatum* as an entomopathogen: development of a fungal bioinsecticide against cotton leafworm (*Spodoptera littoralis*). Microbiol Res 270:127334. https://doi.org/10.1016/j.micres.2023.127334

Liang Y, Wang J, Zhang X, Li K, Su J, Gui M et al (2024) Comprehensive phytohormone metabolomic and transcriptomic analysis of tobacco (*Nicotiana tabacum*) infected by tomato spotted wilt virus (TSWV). Virus Res 342:199334. https://doi.org/10.1016/j.virusres.2024.199334

Lim GH, Singhal R, Kachroo A, Kachroo P (2017) Fatty acid– and lipid-mediated signaling in plant defense. Annu Rev

Phytopathol 55:505–536. https://doi.org/10.1146/annurev-phyto-080516-035406
Liu L, Free SJ (2016) Characterization of the *Sclerotinia sclerotiorum* cell wall proteome. Mol Plant Pathol 17:985–995. https://doi.org/10.1111/mpp.12352
Liu J, Zuo R, He Y, Zhou C, Yang L, Gill RA et al (2022) Analysis of tissue-specific defense responses to *Sclerotinia sclerotiorum* in *Brassica napus*. Plants 11:2001. https://doi.org/10.3390/plants11152001
Lodi RS, Peng C, Dong X, Deng P, Peng L (2023) *Trichoderma hamatum* and its benefits. J Fungi 9:994. https://doi.org/10.3390/jof9100994
Macioszek VK, Jęcz T, Ciereszko I, Kononowicz AK (2023) Jasmonic acid as a mediator in plant response to necrotrophic fungi. Cells 12:1027. https://doi.org/10.3390/cells12071027
Madloo P, Lema M, Cartea ME, Soengas P (2021) *Sclerotinia sclerotiorum* response to long exposure to glucosinolate hydrolysis products by transcriptomic approach. Microbiol Spectr 9:10–1128. https://doi.org/10.1128/Spectrum.00180-21
Maurya S, Ntakirutimana R, Debnath B, Rana M, Kaushik D, Srivastava S (2024) *Trichoderma* and their secondary metabolites–a potential approach in plant disease management. Biopestic Int 20:21–33. https://doi.org/10.2174/1874437001408010127
Meena M, Yadav G, Sonigra P, Nagda A, Mehta T, Swapnil P, Marwal A (2022) Role of elicitors to initiate the induction of systemic resistance in plants to biotic stress. Plant Stress 5:100103. https://doi.org/10.1016/j.stress.2022.100103
Mukherjee PK, Mendoza-Mendoza A, Zeilinger S, Horwitz BA (2022) Mycoparasitism as a mechanism of *Trichoderma*-mediated suppression of plant diseases. Fungal Biol Rev 39:15–33. https://doi.org/10.1016/j.fbr.2021.11.004
O'Sullivan CA, Belt K, Thatcher LF (2021) Tackling control of a cosmopolitan phytopathogen: *Sclerotinia*. Front Plant Sci 12:707509. https://doi.org/10.3389/fpls.2021.707509
Ojaghian S, Wang L, Zhang L (2020) Expression of lytic enzyme genes involved in antagonistic activity of *Trichoderma viridescens* during interaction with *Sclerotinia sclerotiorum*. Eur J Plant Pathol 157:223–226. https://doi.org/10.1007/s10658-020-01992-0
Perrot T, Pauly M, Ramírez V (2022) Emerging roles of β-glucanases in plant development and adaptative responses. Plants 11:1119. https://doi.org/10.3390/plants11091119
Poveda J (2021) *Trichoderma* as biocontrol agent against pests: new uses for a mycoparasite. Biol Control 159:104634. https://doi.org/10.1016/j.biocontrol.2021.104634
Poveda J, Díez-Méndez A (2023) Use of elicitors from macroalgae and microalgae in the management of pests and diseases in agriculture. Phytoparasitica 51:667–701. https://doi.org/10.1007/s12600-022-01009-y
Poveda J, Zabalgogeazcoa I, Soengas P, Rodríguez VM, Cartea ME, Abilleira R, Velasco P (2020) *Brassica oleracea* var. *acephala* (kale) improvement by biological activity of root endophytic fungi. Sci Rep 10:20224. https://doi.org/10.1038/s41598-020-77215-7
Poveda J, Velasco P, de Haro A, Johansen TJ, McAlvay AC, Möllers C et al (2021) Agronomic and metabolomic side-effects of a divergent selection for indol-3-ylmethylglucosinolate content in kale (*Brassica oleracea* var. *acephala*). Metabolites 11:384. https://doi.org/10.3390/metabo11060384
Poveda J, Díaz-González S, Díaz-Urbano M, Velasco P, Sacristán S (2022) Fungal endophytes of Brassicaceae: molecular interactions and crop benefits. Front Plant Sci 13:932288. https://doi.org/10.3389/fpls.2022.932288
Poveda J, Rodríguez VM, Abilleira R, Velasco P (2023) *Trichoderma hamatum* can act as an inter-plant communicator of foliar pathogen infections by colonizing the roots of nearby plants: a new inter-plant "wired communication." Plant Sci 330:111664. https://doi.org/10.1016/j.plantsci.2023.111664
Priyashantha AH, Dai DQ, Bhat DJ, Stephenson SL, Promputtha I, Kaushik P et al (2023) Plant–fungi interactions: where it goes? Biology 12:809. https://doi.org/10.3390/biology12060809
Pushpalatha HG, Mythrashree SR, Shetty R, Geetha NP, Sharathchandra RG, Amruthesh KN, Shetty HS (2007) Ability of vitamins to induce downy mildew disease resistance and growth promotion in pearl millet. Crop Prot 26:1674–1681. https://doi.org/10.1016/j.cropro.2007.02.012
Riseh RS, Vazvani MG, Kennedy JF (2023) β–glucan-induced disease resistance in plants: a review. Int J Biol Macromol 253:127043. https://doi.org/10.1016/j.ijbiomac.2023.127043
Rodríguez VM, Velasco P, Cartea ME, Poveda J (2023) Systemic biochemical changes in pepper (*Capsicum annuum* L.) against *Rhizoctonia solani* by kale (*Brassica oleracea* var. *acephala* L.) green manure application. BMC Plant Biol 23:515. https://doi.org/10.1186/s12870-023-04525-z
Ruiz-Herrera J, Ortiz-Castellanos L (2019) Cell wall glucans of fungi. A review. The Cell Surface 5:100022. https://doi.org/10.1016/j.tcsw.2019.100022
Saharan GS, Mehta NK, Meena PD, Saharan GS, Mehta NK, Meena PD (2021) Biometabolomics of host resistance to hemi-biotrophs and necrotrophs. In: Saharan GS, Mehta NK, Meena PD (eds) Molecular Mechanism of Crucifer's Host-Resistance. Springer, Berlin, Germany, pp 495–584
Shahbazi S, Askari H, Alizadeh M (2025) Cell wall degradation by glucanase activity: *Trichoderma pleuroticola* and *Pythium ultimum* interaction. Biocatal Agric Biotechnol. https://doi.org/10.1016/j.bcab.2025.103643
Shang Q, Jiang D, Xie J, Cheng J, Xiao X (2024) The schizotrophic lifestyle of *Sclerotinia sclerotiorum*. Mol Plant Pathol 25:e13423. https://doi.org/10.1111/mpp.13423
Stasińska-Jakubas M, Hawrylak-Nowak B (2022) Protective, biostimulating, and eliciting effects of chitosan and its derivatives on crop plants. Molecules 27:2801. https://doi.org/10.3390/molecules27092801
TariqJaveed M, Farooq T, Al-Hazmi AS, Hussain MD, Rehman AU (2021) Role of *Trichoderma* as a biocontrol agent (BCA) of phytoparasitic nematodes and plant growth inducer. J Invertebr Pathol 183:107626. https://doi.org/10.1016/j.jip.2021.107626
Teng Z, Yu Y, Zhu Z, Hong SB, Yang B, Zang Y (2021a) Melatonin elevated *Sclerotinia sclerotiorum* resistance via modulation of ATP and glucosinolate biosynthesis in *Brassica rapa* ssp. *pekinensis*. J Proteomics 243:104264. https://doi.org/10.1016/j.jprot.2021.104264
Teng Z, Zheng W, Yu Y, Hong SB, Zhu Z, Zang Y (2021b) Effects of BrMYC2/3/4 on plant development,

glucosinolate metabolism, and *Sclerotinia sclerotiorum* resistance in transgenic *Arabidopsis thaliana*. Front Plant Sci 12:707054. https://doi.org/10.3389/fpls.2021.707054

Tomah AA, Khattak AA, Aldarraji MH, Al-Maidi AAH, Mohany M, Al-Rejaie SS, Ogunyemi SO (2024) Sclerotia degradation by *Trichoderma*-mycoparasitic; an effective and sustainable trend in the drop lettuce disease control caused by *Sclerotinia sclerotiorum*. Arch Microbiol 206:286. https://doi.org/10.1007/s00203-024-04014-3

Troian RF, Steindorff AS, Ramada MHS, Arruda W, Ulhoa CJ (2014) Mycoparasitism studies of *Trichoderma harzianum* against *Sclerotinia sclerotiorum*: evaluation of antagonism and expression of cell wall-degrading enzymes genes. Biotechnol Lett 36:2095–2101. https://doi.org/10.1007/s10529-014-1583-5

Velasco P, Rodríguez VM, Soengas P, Poveda J (2021) *Trichoderma hamatum* increases productivity, glucosinolate content and antioxidant potential of different leafy brassica vegetables. Plants 10:2449. https://doi.org/10.3390/plants10112449

Wang Y, Wang J, Wang W (2024) Identification of mycoparasitism-related genes in *Trichoderma harzianum* T4 that are active against *Colletotrichum musae*. Arch Microbiol 206:29. https://doi.org/10.1007/s00203-023-03767-7

Zantinge JL, Huang HC, Cheng KJ (2002) Microplate diffusion assay for screening of β-glucanase-producing microorganisms. Biotechniques 33:798–806. https://doi.org/10.2144/02334st03